Isoform-Specific Effects of Charged Residues at Borders of the M1−M2 Loop of the Na,K-ATPase α Subunit†

Maddalena V. Coppi,*,‡ Leigh A. Compton,§ and Guido Guidotti||

Department of Microbiology, University of Massachusetts, Amherst, Massachusetts 01003, Centenary College of Louisiana, 2911 Centenary Boulevard, Shreveport, Louisiana 71134, and Department of Molecular and Cellular Biology, Harvard University, 7 Divinity Avenue, Cambridge, Massachusetts 02138

Received September 10, 1998; Revised Manuscript Received December 11, 1998

ABSTRACT: The Na,K-ATPase is specifically inhibited by the cardiac glycoside, ouabain. Via a largely undefined mechanism, the ouabain affinity of the Na,K-ATPase can be manipulated by mutating the residues at the borders of the first extracellular (M1−M2) loop of the α subunit [Price, E. M., Rice, D. A., and Lingrel, J. B. (1990) *J. Biol. Chem. 265*, 6638−6641]. To address this issue, we compared the effects of two combinations of charged residues at the M1−M2 loop border, R113,D124 and D113,R124 (numbered according to the rat α1 subunit), on the ouabain sensitivity of the α1 and α2 isoforms. We report that ouabain sensitivity is dependent not only upon the identity of the residues at the M1−M2 loop border but also upon the context into which they are introduced. Furthermore, at low concentrations of ATP, the identity of the residues at the M1−M2 loop border affects the regulation of ATP hydrolysis by potassium in an isoform-specific manner. Analysis of chimeric α subunits reveals that the effects of potassium are determined primarily by the interaction of the N-terminus and M1−M2 loop with the C-terminal third of the α subunit. M1−M2 loop border residues may, therefore, influence ouabain sensitivity indirectly by altering the stability or structure of the intermediate of the Na,K-ATPase catalytic cycle which is competent to bind ouabain.

The Na,K-ATPase[1] both maintains and establishes the electrochemical gradients present across the plasma membrane of mammalian cells by catalyzing the ATP-dependent transport of sodium and potassium ions (*1*). It is an oligomeric integral membrane protein consisting of two major subunits, α and *β*, of which there are several isoforms, and a third small proteolipid *γ* subunit (*2*). The 100 kDa α subunit comprises 10 putative membrane-spanning segments, M1−M10, and a large intracellular loop containing the nucleotide binding site and catalytic aspartyl residue. The 40−60 kDa *β* subunit consists of a short cytoplasmic strand, a single membrane-spanning segment, and a glycosylated extracellular domain (*1*). The cation occlusion site of the Na,K-ATPase is thought to be formed by multiple residues located in the membrane-spanning segments of the α and *β* subunits (*3*). The ∼6.5 kDa *γ* subunit has been shown to play a role in modulating K^+ activation of the Na,K-ATPase (*2*). During catalysis, the Na,K-ATPase alternates between two distinct conformational states, E1 and E2. Interconversion between E1 and E2 is intimately linked both to nucleotide binding and hydrolysis and to cation binding and occlusion (*4*). These conformational states can be distinguished by their dissimilar affinities for phosphate, nucleotides, and the specific inhibitor of the Na,K-ATPase, ouabain (*4*).

Ouabain is thought to inhibit the Na,K-ATPase by binding the extracellular and intramembrane surfaces of the enzyme when it is in the E2 conformation, thereby preventing regeneration of the E1 conformation and catalysis (*1*, *4*). The sensitivity of the Na,K-ATPase to inhibition by ouabain appears to be determined exclusively by the identity of the α subunit (*1*). Naturally occurring α subunits yield Na,K-ATPase molecules which vary dramatically in ouabain sensitivity, with K_i's ranging from 1×10^{-7} M [sheep α1 (*5*), rat α2 (*6*), and rat α3 (*6*)] to 1×10^{-4} M ouabain [rat α1 (*7*)]. One strategy used to identify the amino acids involved in the interaction between ouabain and the α subunit is to mutagenize ouabain-sensitive α1 subunits (K_i in the 1×10^{-7} M range) and then to screen mutants for their ability to confer ouabain resistance upon ouabain-sensitive cell lines (*7*). Using this approach, 16 residues scattered throughout the extracellular surface and membrane-spanning segments

† This work was carried out at the Department of Molecular Biology, Harvard University (7 Divinity Ave., Cambridge, MA 02138), and supported by Grants DK27626 and HL08893 from the NIH. M.V.C. was partially funded by NIH Training Grant GM07598. L.A.C. was the recipient of a Howard Hughes Medical Institute Summer Research Internship at Harvard University.

* To whom correspondence should be addressed: Department of Microbiology, University of Massachusetts, 203 N Morrill 4N, Amherst, MA 01003. Phone: (413) 545-9647. Fax: (413) 545-1578. E-mail: mcoppi@microbio.umass.edu.

‡ University of Massachusetts.

§ Centenary College of Louisiana.

|| Harvard University.

[1] Abbreviations: Na,K-ATPase, sodium−potassium adenosine triphosphatase; M1−M2 loop, extracellular loop connecting the first and second membrane-spanning segments of the Na,K-ATPase α subunit; SE, standard error; SD, standard deviation; Tris, tris(hydroxymethyl)-aminoethane; Tris-ATP, ATP buffered with Tris; bp, base pair; PCR, polymerase chain reaction; P_i, inorganic phosphate; K_i, concentration of inhibitor at which 50% of the Na,K-ATPase activity is inhibited; V_{max}, maximal enzymatic activity; N-terminus, amino terminus; C-terminus, carboxyl terminus.

10.1021/bi982180j CCC: $18.00
Published on Web 02/05/1999

of the α subunit have been identified as determinants of ouabain sensitivity [reviewed by Croyle et al. (*8*)]. Thirteen of these residues are conserved in the sheep α1 subunit (*9*) and in all three rat α subunits (*10*).

There is convincing evidence for a direct contact with ouabain for only one of the 16 residues identified as determinants of ouabain sensitivity by α subunit mutagenesis. Cys 104 [sheep α1 (*9*)], a conserved residue in M1, is thought to interact with the steroid nucleus of ouabain via a hydrogen bond (*11*−*14*). Mutagenesis of the remaining 15 residues could potentially alter ouabain binding indirectly, either by changing the orientation or properties of residues which normally contact ouabain, by causing side chains to protrude into the ouabain binding cleft, or by altering the E1−E2 equilibrium (*15*, *16*). Site-directed mutagenesis (reviewed in refs *17* and *18*) and biochemical studies (reviewed in ref *3*) have implicated residues in M4−M10 in cation binding and occlusion. Thus mutagenesis of residues in or adjacent to these membrane-spanning segments may influence ouabain binding indirectly as a consequence of alterations in cation binding (*8*). In fact, mutagenesis of a leucine residue in the extracellular M5−M6 loop simultaneously decreased ouabain sensitivity and increased apparent potassium affinity (*19*). The hairpin formed by M1, M2, and the extracellular M1−M2 loop is another region where mutations have the potential to alter ouabain binding indirectly. This hairpin links two cytoplasmic domains thought to play a role in modulating ATP binding and regulating the E1−E2 conformational equilibrium (*20*−*23*).

Because they differ in ouabain-resistant and ouabain-sensitive α subunits (*10*), the two residues at the borders of the M1−M2 loop [positions 113 and 124 of rat α1 (*9*)] have been the subject of considerable study. Furthermore, the K_i of three different ouabain-sensitive α subunits can be changed to values similar to that of the highly resistant rat α1 subunit ($K_i = \sim 1 \times 10^{-4}$ M) simply by substituting their M1−M2 loop border residues with those of rat α1 (*7*, *24*). Mutations at the M1−M2 loop border decrease ouabain sensitivity by increasing the dissociation rate of the inhibitor (*13*). However, the mechanism by which M1−M2 loop border residues influence this rate is not well understood. Although the presence of charged residues at the M1−M2 loop border seems to be critical for ouabain resistance, there is no clear correlation between the type of charged residue present and the degree of ouabain resistance (*5*). This result suggests that the M1−M2 loop border residues may influence ouabain affinity indirectly via their interaction with other as yet uncharacterized residues. This view is further supported by the observation that a monoclonal antibody, which specifically binds the M1−M2 loop, enhances rather than blocks ouabain binding (*25*). Finally, although the sugar moiety of cardiac glycosides greatly affects their rate of dissociation, the M1−M2 loop border residues do not appear to interact with this moiety (*26*).

Here we report that the effect of particular residues at the M1−M2 loop border upon ouabain affinity is context-dependent. In addition, we present evidence that the M1−M2 loop border residues can affect the kinetic properties of both the α1 and α2 isoforms of the rat Na,K-ATPase. Our data further support the hypothesis that the effects of the M1−M2 border residues on ouabain affinity involve their interaction with other α subunit residues and point to a potential role for the M1−M2 loop in the regulation of the E1−E2 equilibrium.

EXPERIMENTAL PROCEDURES

Materials. All reagents used to culture HeLa cells were purchased from GibcoBRL (Grand Island, NY). All chemicals used were reagent grade or better. [γ-^{32}P]ATP was obtained from Dupont-NEN (Boston, MA). Ouabain and Tris-ATP were purchased from Sigma Chemical Co. (St. Louis, MO). The vector rα1-pkC4 (*7*) and a version of the vector rα2-pkC4 (*24*), which was wild type at positions 111 and 122, were obtained from J. Lingrel (University of Cincinnati, Cincinnati, OH). The mammalian expression vector pMT2 (*27*) was obtained with the permission of the Genetics Institute (Cambridge, MA), and the mammalian expression vector pcDNA3 was purchased from Invitrogen (San Diego, CA).

Molecular Biology. Alignment of the α1 and α2 sequences [numbering according to Shull et al. (*10*)] revealed two conserved restriction sites at analogous positions: an *Afl*III site located near the phosphorylated aspartyl residue (rat α1, bp 1406, H386; rat α2, bp 1261, H384) and an *Nco*I site in M5 (rat α1, bp 2435, A729; rat α2, bp 2287, A727). By altering two nucleotides of the α1 subunit, it was possible to create a third common restriction site, *Nhe*I, at the N-terminus of M2 (rat α1, bp 643, flanked by V130 and L131; rat α2, bp 497, flanked by V128 and L129). Creation of the α1 subunit *Nhe*I site resulted in the substitution S132A, alanine being the residue found at the corresponding position of the α2 subunit.

The expression vector pMT2α2**RD**, which directs expression of the rat α2L111R,N122D (α2**RD**) subunit, was constructed as previously described (*28*). To facilitate construction of the various mutant and chimeric α2 subunits, the complete α2**RD** cDNA was excised from pMT2α2**RD** and ligated into the *Pst*I site of pGem3zf− (Promega, Madison, WI). The substitutions L111D and N122R were introduced into an N-terminal restriction fragment of the α2 subunit by the method of Kunkel et al. (*29*). A *Hin*dIII−*Nhe*I fragment containing these substitutions was substituted for the corresponding piece of α2**RD** to generate the complete α2**DR** coding sequence. Subsequently, PCR was used to generate a *Hin*dIII−*Nhe*I restriction fragment of α2**DR** in which the 5′ untranslated sequence was replaced by a consensus Kozak sequence (*30*). The sense primer was 5′-GGG-AAGCTT-GCCGCCACC-ATG-GGA-CGT-GGG-GCA-GGG-CGT-3′ and encoded the N-terminal amino acids MGRGAGR preceded by a GC clamp, a *Hin*dIII site, and a consensus Kozak sequence. The antisense primer was 5′-CC-GC-TAG-CAC-GAT-ACC-TAG-ATA-3′ and complemented the amino acid sequence YLGIVLA. The resulting PCR product was ligated to the remainder of the α2 coding sequence to generate the full-length α2ck**DR** coding sequence.

To facilitate further manipulation of the α1**RD** subunit, the rat α1 subunit cDNA and adjoining polylinker were excised from rα1-pkC4 (*7*) and ligated into the *Hin*dIII site of pGem3zf−. A novel *Nhe*I site at bp 643 was introduced into an N-terminal restriction fragment of the α1 subunit by the method of Kunkel et al. (*29*). An *Apa*I−*Bst*BI fragment containing the novel *Nhe*I site was substituted for the

corresponding piece of the wild type α1 subunit to generate the complete α1**RD**NheI(S132A) coding sequence. PCR was used to generate a *Hin*dIII−*Nhe*I restriction fragment consisting of a consensus Kozak sequence followed by the N-terminus of the α1 subunit coding sequence containing the substitutions R113D, D124R, and S132A. The sense primer consisted of a GC clamp followed by a *Hin*dIII site, a consensus Kozak sequence, and the first three amino acids of the rat α1 coding sequence, MGK. Its nucleotide sequence was 5′-GGG-AAGCTT-GCCGCCACC-ATG-GGG-AAG-G-3′. The antisense primer complemented the amino acid sequence AYGIDSATEEEPPNDRLYLGVVLA. Its sequence was 5′-CCGC-TAG-CAC-GAC-CCC-GAG-GTA-CAG-TCG-ATC-ATT-TGG-TGG-TTC-CTC-TTC-TGT-AGC-ACT-ATC-GAT-GCC-ATA-AG-3′. The resulting PCR product was ligated to the remainder of the α1**RD**NheI coding sequence to generate the full-length α1ck**DR**NheI coding sequence.

Following their assembly, the various mutant and chimeric α subunits were introduced into one of two mammalian expression vectors, pMT2 [α2**RD**, α2**DR**, α1**RD**NheI, α2**RD**Nhe1α1, α1**RD**NcoIα2, α2**RD**NheIα1NcoIα2, and α1**RD**(NheI)AflIIα2NcoIα1] or pcDNA3 [α2ck**DR**, α2ck-**DR**NheIα1, α1ck**DR**NheI, and α1ck**DR**NheIα2].

Tissue Culture and Transfection. HeLa cells were cultured at 37 °C and 5% CO_2 in Dulbecco's Modified Eagle's Medium supplemented with penicillin, streptomycin, glutamine, and 10% fetal bovine serum. HeLa cells were transfected by the calcium phosphate method as previously described (*28*). After 2−4 weeks of growth in selective media containing 1 μM ouabain, ouabain-resistant colonies were either stained with crystal violet for counting or cultured individually to generate ouabain-resistant cell lines. All ouabain-resistant cell lines were maintained in medium containing 1 μM ouabain.

Membrane Preparations. All membrane preparations were aliquotted, flash-frozen, and stored at −70 °C. The protein concentration was determined according to the method of Peterson (*31*). Rat skeletal muscle membranes were prepared according to the method of Barchi et al. (*32*). Following a crude dissection to enrich for the outer medulla, rat kidney microsomes were prepared and SDS extracted according to the method of Jørgensen (*33*). Crude membranes from the various HeLa cell lines were prepared according to the method of Jewell and Lingrel (*24*) with the following modifications. After NaI extraction, the membrane pellets were resuspended in wash buffer containing 10 mM Hepes/Tris (pH 7.5) and 0.2 mM EDTA/Tris. After repelleting, the membranes were resuspended in 2−3 mL of wash buffer and dialyzed for at least 24 h against 4 L of 10 mM Hepes/Tris (pH 7.4) to eliminate any residual sodium. The dialyzed membranes were then diluted in wash buffer, pelleted, and resuspended in the same buffer.

Na,K-ATPase Assays. Na,K-ATPase activity was determined as the rate of P_i release from ATP that was either ouabain-inhibitable or sodium-dependent. The use of Tris-ATP enabled measurement of the rate of ATP hydrolysis in the absence of sodium. Incubation times and membrane concentrations were adjusted such that the rate of ATP hydrolysis remained linear (less than 25% of the total ATP hydrolyzed) throughout. For the ouabain titrations shown in Figure 2, Na,K-ATPase activity was measured at 37 °C in buffer containing 2.5 mM ATP, 3 mM $MgCl_2$, 100 mM NaCl or choline chloride, 20 mM KCl, 50 mM Tris/HCl (pH 7.4), 1 mM EGTA, and varying concentrations of ouabain. Membranes were pre-equilibrated with ouabain for 20 min at 37 °C in the absence of KCl and ATP, and the ATPase reaction was initiated by the simultaneous addition of KCl and ATP. The rate of release of P_i was measured according to the method of Lanzetta et al. (*34*). Na,K-ATPase activity in the presence of 1 μM ATP was measured at 37 °C in buffer containing 1 mM $MgCl_2$, 100 mM NaCl or choline chloride, 0.0−5 mM KCl or choline chloride, 50 mM Tris/HCl (pH 7.4), 1 mM EGTA, and an appropriate concentration of ouabain. Membranes were pre-equilibrated for 20 min at 37 °C in the absence of ATP, and the ATPase reaction was initiated by the addition of [γ-^{32}P]ATP/ATP. The rate of release of P_i from [γ-^{32}P]ATP/ATP was measured according to the method of Pressley et al. (*35*) with the following modifications. Trichloroacetic acid was substituted for perchloric acid, and the organic phosphomolybdate complex was extracted into a 1:1 mixture of ethyl acetate and isobutanol.

RESULTS

*Capacity of Various α**DR** and α**RD** Subunits To Support Growth of Ouabain-Resistant Colonies.* Two combinations of charged M1−M2 loop border residues, R114,D124 (**RD**, numbering refers to the rat α1 subunit) and D114,R124 (**DR**), were introduced into rat α1, α2, and chimeric α1−α2 subunits. We chose the **RD** combination, because it occurs naturally in the ouabain-resistant rat α1 subunit (*10*). The combination **DR** was selected for its capacity to turn the sheep α1 isoform into a "super ouabain resistant" enzyme with a K_i in the millimolar range (*5*).

To create the various chimeric α subunits shown in Figure 1, we exploited a naturally occurring *Nhe*I restriction site which cleaves the α2 subunit cDNA at the N-terminus of M2 (bp 497, flanked by V128 and L129). Alignment of the α1 and α2 sequences reveals that mutagenesis of two base pairs in the α1 subunit sequence creates an analogous *Nhe*I site (bp 643, flanked by V130 and L131). Creation of the α1 subunit *Nhe*I site also results in the substitution S132A, alanine being the residue found at the corresponding position of the α2 subunit.

The endogenous α1 subunit of HeLa cells, α1**QN**, has a high affinity for ouabain and can be fully inhibited by micromolar concentrations of the inhibitor. Exogenously expressed ouabain-resistant α subunits such as rat α1**RD** (*5*) and α2**RD** (*24*) can assemble with the endogenous β1 subunit of HeLa cells and enable them to grow at normally toxic concentrations of ouabain. We began by investigating the capacity of the various mutant and chimeric α-subunits shown in Figure 1 to support the growth of ouabain-resistant colonies of HeLa cells. As shown in Figure 1, expression of the α1 subunit containing the novel *Nhe*I site (α1**RD**NheI), α2**RD**, or α2**RD**NheIα1, a chimeric subunit consisting of the N-terminus of the α2**RD** subunit joined to the C-terminus of the α1 subunit, yields hundreds of ouabain-resistant colonies.

Surprisingly, expression of α subunits with the M1−M2 loop border residues **DR** consistently yields fewer ouabain-resistant colonies than the corresponding subunits with **RD** at the loop borders (Figure 1). The number of ouabain-resistant colonies generated by expression of α1ck**DR**NheI,

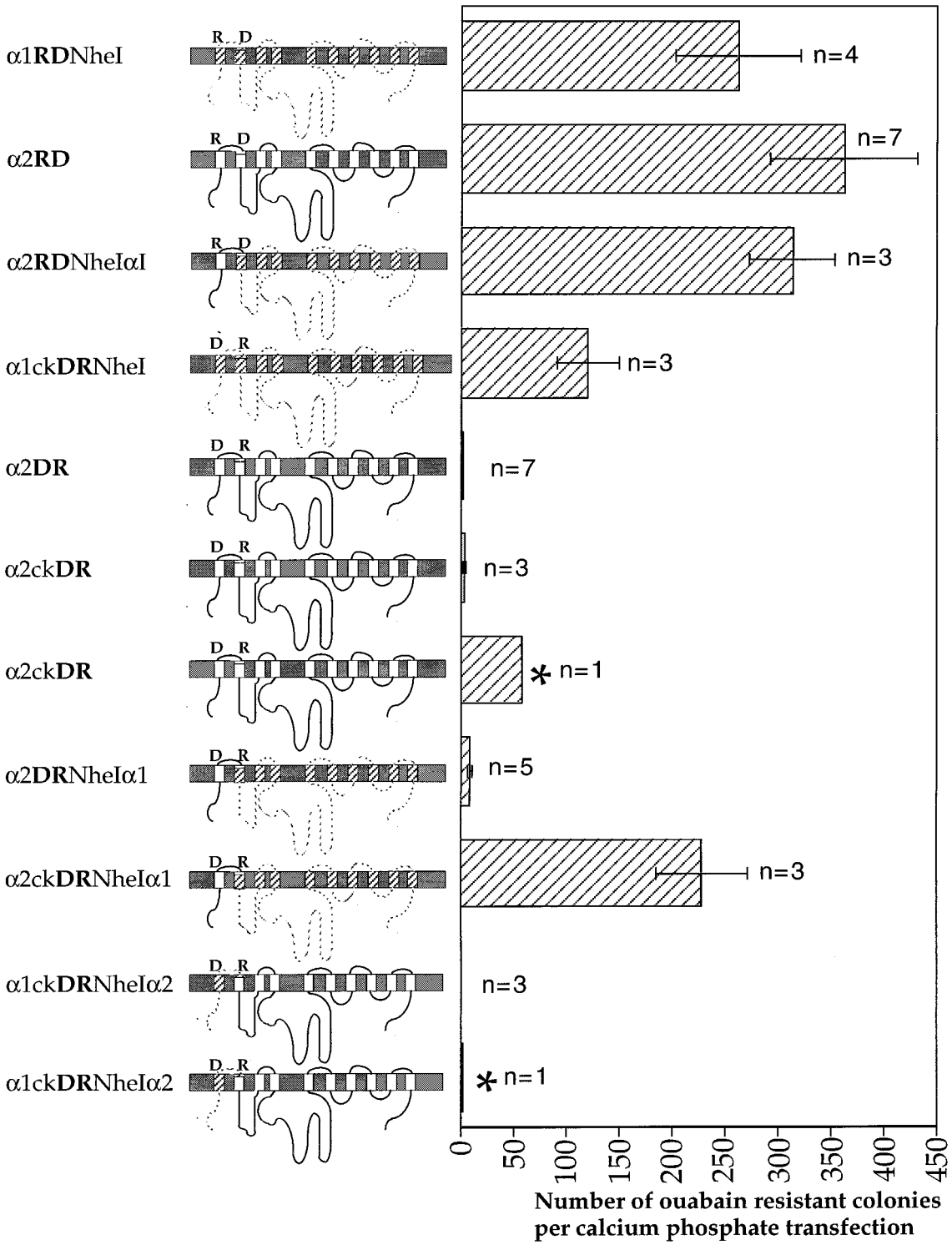

FIGURE 1: Ability of rat α1, rat α2, and chimeric α subunits with substitutions at the borders of the M1−M2 loop to support growth of ouabain-resistant colonies. HeLa cells were transfected with vectors directing expression of the various α subunits by the calcium phosphate method as described in Experimental Procedures. Following either 2 (α1**RD**NheI, α2**RD**, and α2RDNheI) or 3 weeks (remaining α subunits) of growth in medium containing 1 μM ouabain, ouabain-resistant colonies were stained with crystal violet and counted. Data shown are as means ± SE. An asterisk indicates that transfected HeLa cells were cultured in medium containing 10-fold less ouabain (0.1 μM). The nomenclature of the various α subunits is as follows. The residues at the M1−M2 loop borders are indicated in boldface type. The letters "ck" indicate that the 5′ untranslated sequence was replaced by a consensus Kozak sequence (*30*). "NheI" refers to either the restriction site used to fuse the N- and C-termini of the various chimeric α subunits or the presence of a novel *Nhe*I restriction site and resulting S132A substitution in the α1 subunit cDNA. Solid lines and white rectangles denote α2 subunit sequences. Cross-hatched lines and rectangles denote α1 subunit sequences.

α2**DR**NheIα1, and α2**DR** was 45.98 ± 15.40%, 2.62 ± 0.66%, and 0.24 ± 0.16%, respectively, of the number of colonies generated by expression of their **RD** counterparts. The few ouabain-resistant colonies of HeLa cells generated by α2**DR** expression grew so slowly in the presence of 1 μM ouabain that further culturing was not feasible. However, there was abundant α2**DR** expression in the absence of ouabain in transiently transfected COS-7 cells (data not

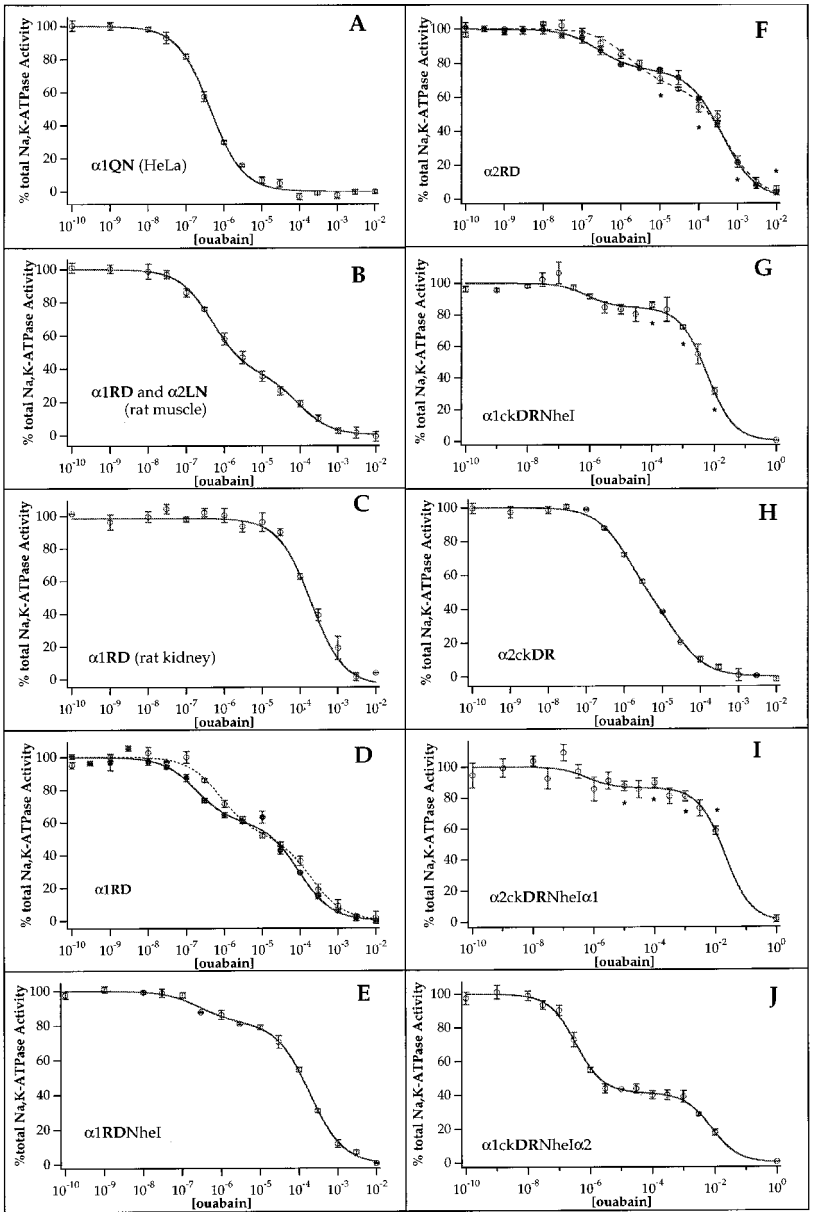

FIGURE 2: Determination of ouabain sensitivity of various α subunits. The nomenclature of α subunits is identical to that described in Figure 1. Na,K-ATPase activity was measured in buffer containing 2.5 mM ATP, 100 mM NaCl, 20 mM KCl, 3 mM $MgCl_2$, 50 mM Tris/HCl (pH 7.4 and 37 °C), 1 mM EGTA, and the indicated concentration of ouabain as described in Experimental Procedures. Raw data were least-squares fitted to either a one-component or a two-component inhibition curve with the program Igor (Wavemetrics, Lake Oswego, OR). To fit the data for membranes prepared from HeLa cells expressing "super ouabain resistant" α subunits (G, I, and J), ATPase activity in the absence of sodium was considered to be equivalent to ATPase activity in the presence of 1 M ouabain. Single-component curves (A and C) were fitted to the function $c = c_o[1 - x/(c_1 + x)] + c_2$, where c is the total Na,K-ATPase activity, x is the ouabain concentration, c_1 is the K_i for ouabain, and c_2 is the ouabain-resistant ATPase activity. Two-component curves (B and D−J) were fitted to the function $c = c_o[1 - [x/(c_1 + x)]c_2 - (x/c_3 + x)(1 - c_2)] + c_4$, where c is the total Na,K-ATPase activity, x is the ouabain concentration, c_1 is the K_i for ouabain of the high-affinity component, c_2 is the fraction of the total Na,K-ATPase activity that can be attributed to the high-affinity component, c_3 is the K_i for ouabain of the low-affinity component, and c_4 is the ouabain-resistant Na,K-ATPase activity. Data are plotted as a percentage of the total Na,K-ATPase activity that was defined by the optimal curve fit. Unless otherwise indicated, data plotted are means ± SE of three independent measurements. An asterisk indicates a point is mean ± SE of six independent measurements. Ouabain titrations were performed on membranes prepared from the following. (A) Untransfected HeLa cells expressing only the endogenous α subunit, α1**QN**. Total Na,K-ATPase activity (mean ± SD) = 38.5 ± 0.49 nmol of P_i mg^{-1} min^{-1}. (B) Rat muscle membranes containing α1**RD** and α2**LN**. Total Na,K-ATPase activity = 1665.3 ± 22.5 nmol of P_i mg^{-1} min^{-1}. (C) SDS-extracted rat kidney microsomes expressing α1**RD**. Total Na,K-ATPase activity = 5250.3 ± 136.1 nmol of P_i mg^{-1} min^{-1}. (D) Two different colonies of HeLa cells expressing α1**RD**. Total Na,K-ATPase activity = 17.37 ± 0.39 nmol of P_i mg^{-1} min^{-1} for black circles and 16.44 ± 0.41 nmol of P_i mg^{-1} min^{-1} for white circles. White circles represent data from the membrane preparation used to measure potassium inhibition at 1 μM ATP. (E) HeLa cells expressing α1**RD**NheI. Total Na,K-ATPase activity = 34.14 ± 0.55 nmol of P_i mg^{-1} min^{-1}. (F) Two different colonies of HeLa cells expressing α2**RD**. Total Na,K-ATPase activity = 25.6 ± 0.31 nmol of P_i mg^{-1} min^{-1} for black circles and 19.31 ± 0.41 nmol of P_i mg^{-1} min^{-1} for white circles. White circles represent data from the membrane preparation used to measure the effect of potassium at 1 μM ATP. All asterisks refer to white circles. (G) HeLa cells expressing α1ck**DR**NheI. Total Na,K-ATPase activity = 28.29 ± 1.05 nmol of P_i mg^{-1} min^{-1}. (H) HeLa cells expressing α2ck**DR**. Total Na,K-ATPase activity = 38.27 ± 0.54 nmol of P_i mg^{-1} min^{-1}. (I) HeLa cells expressing α2ck**DR**NheIα1. Total Na,K-ATPase activity = 29.40 ± 1.34 nmol of P_i mg^{-1} min^{-1}. (J) HeLa cells expressing α1ck**DR**NheIα2. Total Na,K-ATPase activity = 21.60 ± 0.56 nmol of P_i mg^{-1} min^{-1}.

shown), demonstrating that the expression vector was competent.

The failure of an α subunit to support efficient growth of HeLa cells in the presence of micromolar ouabain can have several causes. The difference between the ouabain affinity of the α subunit and the endogenous α1**QN** subunit of HeLa cells may be too small to maintain a sufficiently large population of active Na,K-ATPase molecules. Alternatively, the introduction of substitutions into an α subunit may compromise the assembly or catalytic activity of the Na,K-ATPase (*17*). In both of these cases, increasing the level of α subunit expression may generate enough Na,K-ATPase activity to enable cell division in the presence of ouabain.

Examination of the sequence immediately preceding the initiation codon of the α2 subunit revealed a suboptimal Kozak sequence (*10*, *30*). To increase the level of α2**DR** and α2**DR**NheIα1 expression, we substituted the 5′ untranslated region of these cDNAs with a consensus Kozak sequence. As a result of this change, the number of ouabain-resistant colonies resulting from transfection of the α2ck**DR**NheIα1 cDNA (228 ± 42.6) rose to a level comparable to that achieved by transfection of its **RD** counterpart (α2**RD**NheIα1, 313.0 ± 40.5). This result indicates that an increase in the expression level of the α2**DR**NheIα1 subunit is sufficient to overcome the alterations in either ouabain affinity or enzymatic activity caused by the **DR** mutations. This is not the case for α2ck**DR**, where the number of colonies remains low despite introduction of a consensus Kozak sequence. Substitution of the 5′ untranslated region of α2**DR** with a consensus Kozak sequence did, however, enable us to successfully culture a few colonies expressing α2ck**DR** in 1 μM ouabain. Surprisingly, decreasing the concentration of ouabain in the selective media from 1 to 0.1 μM increased the number of colonies to 58, suggesting that α2ck**DR**, unlike sheep α1**DR** (*5*), has a fairly high affinity for ouabain.

Despite the presence of a consensus Kozak sequence (*30*), expression of the chimeric α1ck**DR**NheIα2 subunit yielded very few colonies (0.33 ± 0.33, $n = 3$). Decreasing the ouabain concentration in the selective media did not appear to significantly increase the number of ouabain-resistant colonies (2, $n = 1$). Thus, the inability of α1ck**DR**NheIα2 to support efficient growth of ouabain-resistant colonies is probably not due to a high ouabain affinity and may instead be due to a defect in the ability of α1ck**DR**NheIα2 to form functional Na,K-ATPase molecules. The possibility that α1ck**DR**NheIα2 is nonfunctional and that the few colonies obtained may be mutants of the original construct has not been excluded.

*Ouabain Sensitivities of Various α**RD** and α**DR** Subunits.* To better understand the effects of the **RD** and **DR** substitutions, we measured the ouabain sensitivity of the Na,K-ATPase activity present in membrane preparations of HeLa cells expressing the various α subunits and compared it to that of the endogenous α1**QN** subunit of HeLa cells as well as to that of the wild type α1**RD** and α2**LN** subunits (Figure 2 and Table 1). As shown in Figure 2, the Na,K-ATPase activity present in all of the ouabain-resistant HeLa cell lines expressing the various α subunits could best be fit by a two-component inhibition curve in which the ouabain sensitivity of the high-affinity component was consistent with that of the endogenous α1**QN** subunit. The contribution of the endogenous α1**QN** subunit to the total Na,K-ATPase activity in these cell lines varies widely, ranging from 14 to 59% of the total.

Table 1: Context-Dependent Effect of M1−M2 Loop Border Residues on Ouabain Sensitivity[a]

α subunit	membrane source	K_i for ouabain (M)	% total Na,K-ATPase activity
α1**QN**	HeLa cells	$(4.35 \pm 0.30) \times 10^{-7}$	100.0 ± 0.0
α2**LN**	rat muscle	$(4.77 \pm 0.57) \times 10^{-7}$	62.60 ± 1.90
α1**RD**	rat muscle	$(0.894 \pm 0.192) \times 10^{-4}$	37.40 ± 1.90
α1**RD**	rat kidney	$(1.91 \pm 0.24) \times 10^{-4}$	100.0 ± 0.0
α1**RD**	HeLa cells expressing rat cDNA	$(0.920 \pm 0.189) \times 10^{-4}$ [b]	60.23 ± 2.61 [b]
		$(1.93 \pm 0.46) \times 10^{-4}$ [c]	52.06 ± 3.03 [c]
α1**RD**NheI		$(1.89 \pm 0.18) \times 10^{-4}$	81.90 ± 1.50
α2**RD**		$(3.95 \pm 0.30) \times 10^{-4}$ [d]	76.02 ± 0.92 [d]
		$(5.11 \pm 0.86) \times 10^{-4}$ [e]	66.70 ± 2.54 [e]
α1ck**DR**NheI		$(5.85 \pm 0.93) \times 10^{-3}$	84.51 ± 2.22
α2ck**DR**		$(2.39 \pm 0.92) \times 10^{-5}$	44.85 ± 8.99
α2ck**DR**NheIα1		$(2.04 \pm 0.44) \times 10^{-2}$	86.32 ± 2.86
α1ck**DR**NheIα2		$(7.7 \pm 1.60) \times 10^{-3}$	41.23 ± 1.56

[a] The identity of residues at the M1−M2 loop borders is indicated in boldface type. The nomenclature of various α subunits is identical to that in the legend of Figure 1. The K_i for ouabain of the various α subunits was determined as described in the legend of Figure 2. Data are means ± SD. [b] Derived from the data depicted as black circles in Figure 2D. [c] Derived from the data depicted as white circles in Figure 2D. [d] Derived from the data depicted as black circles in Figure 2F. [e] Derived from the data depicted as white circles in Figure 2F.

As shown in Table 1, the identity of the residues at the borders of the M1−M2 loop is not an accurate predictor of ouabain sensitivity. This is particularly evident if we compare the ouabain affinities of the various α**DR** subunits. Similar to sheep α1**DR**, α1ck**DR**NheI yields a "super ouabain resistant enzyme" with a K_i for ouabain in the millimolar range [$(5.85 \pm 0.93) \times 10^{-3}$ M]. In contrast, the α2ck**DR** subunit is relatively ouabain-sensitive; its K_i for ouabain is $(2.39 \pm 0.92) \times 10^{-5}$ M. As shown in Figure 2H, it was difficult to resolve α1**QN** from α2ck**DR** activity. Surprisingly, joining the α2 N-terminus containing the **DR** substitutions to the C-terminus of α1 yields an enzyme (α2ck**DR**NheIα1) which is even more ouabain-resistant [K_i for ouabain of $(2.04 \pm 0.44) \times 10^{-2}$ M] than α1ck**DR**NheI. In contrast, the complementary chimera, α1ck**DR**α2, yielded an enzyme with a K_i for ouabain that was very close to that of α1ck**DR**NheI, $(7.70 \pm 1.60) \times 10^{-3}$ M. There is also a 2-fold difference between the ouabain affinities of the α1**RD** and α2**RD** subunits. α2**RD** [$K_i = (4.53 \pm 0.091) \times 10^{-4}$ M, average of c and d, Table 1] is roughly 2-fold more resistant to ouabain inhibition than either α1**RD** [$K_i = (1.43 \pm 0.50) \times 10^{-4}$ M, average of a and b, Table 1] or α1**RD**NheI [$K_i = (1.89 \pm 0.18) \times 10^{-4}$ M].

Thus, ouabain sensitivity is dependent not only upon the identity of the residues at the M1−M2 loop border but also upon the context into which they are introduced. The fact that the ouabain sensitivity of the chimeric α2ck**DR**NheIα1 subunit is distinct from that of either α2ck**DR** or α1ck**DR**NheI indicates that residues located both C-terminal to and N-terminal to or within the M1−M2 loop are important in determining the effects of substitutions at the borders of the M1−M2 loop upon ouabain sensitivity. It is, therefore, unlikely that the M1−M2 loop border residues are involved in a direct interaction with ouabain.

*Effect of Potassium on α1**QN** and α2**RD** Na,K-ATPase Activity at 1 μM ATP*. Agents which alter the conformational (E1−E2) equilibrium of the Na,K-ATPase also induce changes in ouabain affinity (*15*, *16*). Given the context-dependent effects of M1−M2 loop border residue substitutions upon ouabain sensitivity, we hypothesized that these substitutions might influence ouabain affinity by perturbing the E1−E2 equilibrium. In fact, the M1−M2 loop links two cytoplasmic segments which have been implicated in modulation of the E1−E2 equilibrium: the N-terminus (*21*−*23*, *36*) and the M2−M3 loop (*20*). Truncation of the rat α1**RD** subunit N-terminus and introduction of a point mutation, E233K, into the M2−M3 cytoplasmic loop both result in a shift in the E1−E2 conformational equilibrium toward E1. Both of these alterations also cause the effect of potassium upon Na,K-ATPase activity at low ATP concentrations to switch from inhibition to activation (*20*, *23*). Because changes in the effects of potassium on Na,K-ATPase activity at low ATP concentrations are fairly easy to measure and might indicate perturbations of the E1−E2 equilibrium, we decided to investigate the effects of substitutions of the M1−M2 loop border residues upon this parameter.

To perform this analysis, we needed to be able to separate the effects of potassium on the various mutant and chimeric α subunits from its effects on the α1**QN** activity present in all of our preparations. Previously, this had been attempted by adding a concentration of ouabain (10 μM) which would inhibit α1**QN** without substantially inhibiting ouabain-resistant isoforms. In the presence of 1 μM ATP, 100 mM NaCl, and 0 mM KCl, 10 μM ouabain fully inhibits α1**QN** (data not shown). However, as shown in Figure 3A, the addition of potassium significantly reduces the extent of inhibition of α1**QN** by 10 μM ouabain. In Figure 3B, the apparent α1**QN** activity was calculated by subtracting the rate of ATP hydrolysis in the presence of ouabain from the rate of ATP hydrolysis in the absence of ouabain at each potassium concentration. The resulting potassium inhibition curve (i) is quite different from that of actual α1**QN** activity (ii) which we calculated by subtracting the amount of ATPase activity that was resistant to 10 μM ouabain at 0 mM KCl from the total ATPase activity at each concentration of KCl. The difference between these two curves (iii = ii − i) is equal to the amount of α1**QN** activity that is not inhibited by 10 μM ouabain in the presence of potassium. As shown in Figure 3B, approximately 30% of the α1**QN** activity is not inhibited by 10 μM ouabain in the presence of 5 mM KCl. Thus, the ouabain affinity of α1**QN** at low ATP concentrations is significantly reduced by millimolar concentrations of potassium.

There are therefore two ways to assess the effect of potassium on an α subunit expressed in HeLa cells. One is to measure total Na,K-ATPase activity and then subtract the amount of Na,K-ATPase activity due to α1**QN** at each potassium concentration. The other is to measure Na,K-ATPase activity in the presence of 10 μM ouabain and then subtract the amount of α1**QN** activity that is not inhibited by 10 μM ouabain at each potassium concentration. These two methods require knowledge of both the effect of KCl on α1**QN** activity (Figure 3B) and the ratio of expressed α subunit to α1**QN** activity at 0 mM KCl and 1 μM ATP.

The effect of potassium on the activity of α2**RD** in the presence of 1 μM ATP and 100 mM NaCl is shown in Figure 4. In panel A, we determined that the ratio of α2**RD** to α1**QN** activity in the presence of 1 μM ATP and 0 mM KCl was essentially identical to the ratio of the activity of the two isoforms under V_{max} conditions (Figure 2F). α2**RD** comprises 71.11 ± 1.81% of the total Na,K-ATPase activity at 0 mM KCl and 1 μM ATP (Figure 3A) and 66.70 ± 2.54% of the total Na,K-ATPase activity under V_{max} conditions (Figure 2F and Table 1).

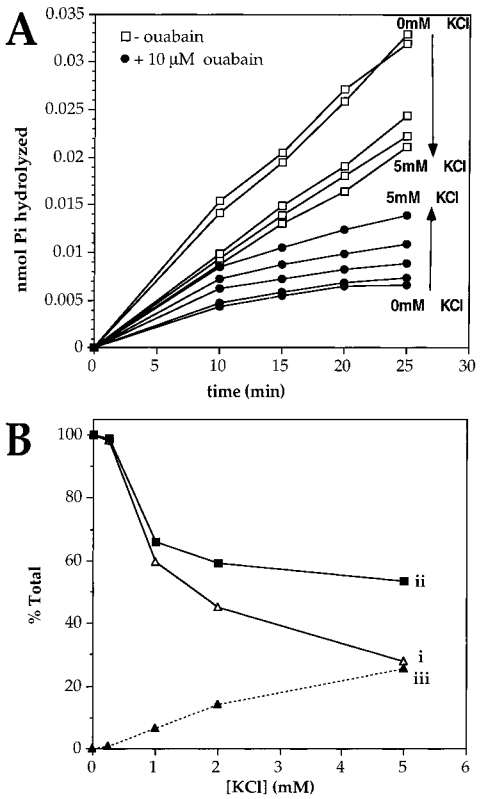

FIGURE 3: Effect of potassium on α1**QN** activity at 1 μM ATP. (A) Effect of 10 μM ouabain and potassium on ATP hydrolysis by membranes prepared from untransfected HeLa cells. The rate of ATP hydrolysis by 1 μg of membranes was measured in the presence of 1 μM ATP, 100 mM NaCl, 50 mM Tris/HCl (pH 7.4 and 37 °C), 1 mM EGTA, 1 mM $MgCl_2$, and 0.0, 0.25, 1.0, 2, and 5 mM KCl as described in Experimental Procedures: (□) ATP hydrolysis in the absence of ouabain and (●) ATP hydrolysis in the presence of 10 μM ouabain. Data are the average of two independent experiments. Data for ATP hydrolysis in the absence of ouabain could be fit to a straight line with an r^2 of ≥0.99. Data for ATP hydrolysis in the presence of ouabain were not linear but could be fit to a power function with an r^2 of ≥0.99. (B) Addition of KCl reduces the extent of inhibition of α1**QN** by 10 μM ouabain. Data shown are calculated for the 25 min time point using curve fits described in part A. In the absence of potassium, α1**QN** was nominally completely inhibited by 10 μM ouabain. In addition, the activity of other ATPases in our membrane preparations was not significantly affected by the addition of KCl (data not shown). (i) % apparent α1**QN** activity. Apparent α1QN activity is defined as the difference between the rate of ATP hydrolysis in the absence and presence of 10 μM ouabain at each KCl concentration (=□ − ● in panel A). (ii) % α1**QN** activity. α1**QN** activity was calculated by subtracting the amount of ATPase activity that was resistant to 10 μM ouabain at 0 mM KCl from the total ATPase activity at various concentrations of KCl. (iii) % α1**QN** activity which is resistant 10 μM ouabain (=ii − i) at various concentrations of KCl.

In Figure 4B, we show the calculation of α2**RD** activity from total Na,K-ATPase activity (i). According to the ouabain titration shown in Figure 4A, in the absence of potassium 28.9% of the total Na,K-ATPase activity is due

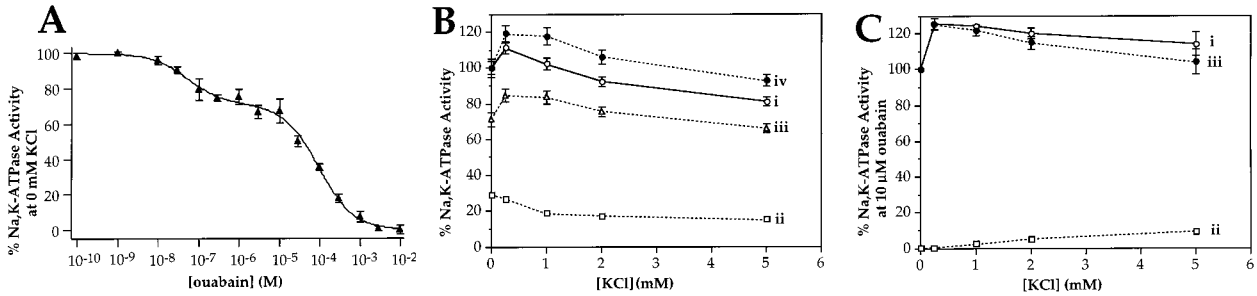

FIGURE 4: Effect of potassium on α2**RD** Na,K-ATPase activity at 1 μM ATP. Membranes were from the same preparation used to generate the data depicted in Figure 2F (○). The rate of ATP hydrolysis at 1 μM ATP was measured as described in Experimental Procedures. (A) Effect of 0 mM KCl and 1 μM ATP on the ratio of α2**RD** to α1**QN** Na,K-ATPase activity in membranes prepared from HeLa cells expressing rat α2**RD**. Raw data were least-squares fitted to a two-component ouabain inhibition curve as described in the legend of Figure 2. Data plotted are means ± SE of three independent measurements, and are plotted as a percentage of the total Na,K-ATPase activity defined by the optimal curve fit [0.663 ± 0.014 nmol of P_i mg^{-1} min^{-1} (mean ± SD)]. (B) α2**RD** activity as a function of KCl concentration, determined from total Na,K-ATPase activity. (i) % total Na,K-ATPase (α1**QN** and α2**RD**) activity, determined by subtracting the amount of ATP hydrolyzed in the absence of sodium from the amount of ATP hydrolyzed in the presence of sodium at each KCl concentration. Data are means ± SE of three independent measurements. The 100% total Na,K-ATPase activity at 0 mM KCl is 0.558 ± 0.016 nmol of P_i mg^{-1} min^{-1}. (ii) % total Na,K-ATPase activity due to α1**QN**. At 0 mM KCl, the % total Na,K-ATPase activity due to α1**QN** was set at 28.9% in accordance with the ouabain titration shown in panel A. This value was multiplied by the fraction of α1**QN** activity in untransfected HeLa cells that was active at each potassium concentration (1 at 0 mM KCl, 0.924 ± 0.156 at 0.25 mM KCl, 0.644 ± 0.181 at 1 mM KCl, 0.5842 ± 0.204 at 2 mM KCl, and 0.516 ± 0.160 at 5 mM KCl). Data are means ± SE of 11 experiments where 100% = 1.131 ± 0.042 nmol of P_i mg^{-1} min^{-1}. (iii) % total Na,K-ATPase activity due to α2**RD**, calculated by subtracting curve ii from curve i. (iv) % α2**RD** activity as a function of KCl concentration, calculated from curve iii by defining the amount of total Na,K-ATPase activity due to α2**RD** at 0 mM KCl as 100%. (C) α2**RD** activity as a function of KCl concentration, determined from the total Na,K-ATPase activity in the presence of 10 μM ouabain. (i) % total Na,K-ATPase (α2**RD** and α1**QN**) activity in the presence of 10 μM ouabain, determined by subtracting the amount of ATP hydrolyzed in the presence of either 0 mM NaCl or 10 mM ouabain from the amount of ATP hydrolyzed in the presence of 100 mM NaCl and 10 μM ouabain at each KCl concentration. Data are means ± SE of nine independent experiments, where 100% is 0.334 ± 0.008 nmol of P_i mg^{-1} min^{-1}. (ii) % total Na,K-ATPase activity at 10 μM ouabain due to α1**QN**. Na,K-ATPase activity at 10 μM ouabain and 0 mM KCl (α2**RD** activity at 0 mM KCl) was multiplied by the ratio of α1**QN** to α2**RD** activity at 0 mM KCl and 0 mM ouabain (0.406, determined from ouabain titration shown in panel A) to determine α1**QN** activity in the absence of potassium and ouabain. This value was subsequently multiplied by the fraction of α1**QN** activity that is resistant to 10 μM ouabain at each KCl concentration (calculated as described in the legend of Figure 3B). (iii) % α2**RD** activity as a function of KCl concentration, calculated by subtracting curve ii from curve i.

to α1**QN**. To calculate the percentage of the total Na,K-ATPase activity due to α1**QN** in the presence of potassium (ii), we assume that α1**QN** in membranes containing α2**RD** is inhibited by potassium to the same extent as α1**QN** in membranes prepared from untransfected HeLa cells. The amount of Na,K-ATPase activity due to α2**RD** (iii) is subsequently calculated by subtracting α1**QN** activity (ii) from the total Na,K-ATPase activity (i). By defining the amount of Na,K-ATPase activity due to α2**RD** at 0 mM KCl as 100% α2**RD** activity, we can then determine α2**RD** activity as a function of potassium concentration (iv).

Figure 4C (i) shows the effect of potassium upon Na,K-ATPase activity in the presence of 10 μM ouabain. In the absence of potassium, α1**QN** is completely inhibited by 10 μM ouabain, and thus, all the Na,K-ATPase activity is due to α2**RD**. By multiplying this quantity by the ratio of α1**QN** to α2**RD** activity in the absence of potassium and ouabain (determined from the titration shown in panel A), we can calculate α1**QN** activity in the absence of potassium and ouabain. To determine how much of this α1**QN** activity is resistant to 10 μM ouabain in the presence of potassium (ii), we performed a calculation analogous to that shown in Figure 3B. The α2**RD** activity as a function of potassium (iii) was subsequently calculated by subtracting α1**QN** activity which was resistant to 10 μM ouabain (ii) from the total Na,K-ATPase activity in the presence of 10 μM ouabain (i).

As shown in Figure 4, the approaches used to derive the data shown in panels B and C yield essentially the same result. As previously reported by Daley et al. (*22*), α2**RD** undergoes a modest activation in response to potassium in the presence of 1 μM ATP. Thus, both approaches appear to be valid methods for determining the effect of potassium on a particular Na,K-ATPase isoform when a mixed population of isoforms is present.

*Effect of Potassium on α1**RD** and α2**LN** Na,K-ATPase Activity at 1 μM ATP*. To determine if the **RD** mutations altered the potassium sensitivity of the α2 isoform at low ATP concentrations, we investigated the effect of potassium on the wild type α2**LN** subunit (Figure 5). We used rat muscle membranes as our source of α2**LN**, because the ouabain sensitivity of α2**LN** [K_i = (4.77 ± 0.57) × 10^{-7} M] precludes selection for its expression in HeLa cells. Both the α1**RD** and α2**LN** isoforms are present in rat muscle membranes (*37*). As shown in Figures 5A and 2B, the ratio of α2**LN** to α1**RD** activity in rat muscle was very similar under suboptimal (1 μM ATP and 0 mM KCl, Figure 5A) and V_{max} conditions (Figure 2F, open circles): 55.32 ± 2.43 versus 62.60 ± 1.90% of the total Na,K-ATPase activity, respectively.

In Figure 5B, α2**LN** activity as a function of KCl concentration (iv) was determined by the method used to derive the data shown in Figure 4B, by measuring the effect of potassium on the total (α1**RD** and α2**LN**) Na,K-ATPase activity (ii) in rat muscle and then subtracting the amount of Na,K-ATPase activity due to α1**RD** (iii) at each potassium concentration. Rat kidney membranes, a source of the purified α1**RD** isoform (*33*), were used to determine how the activity of α1**RD** changes as a function of potassium concentration. As previously reported (*21*), α1**RD** activity (i) was inhibited by the addition of potassium in the presence

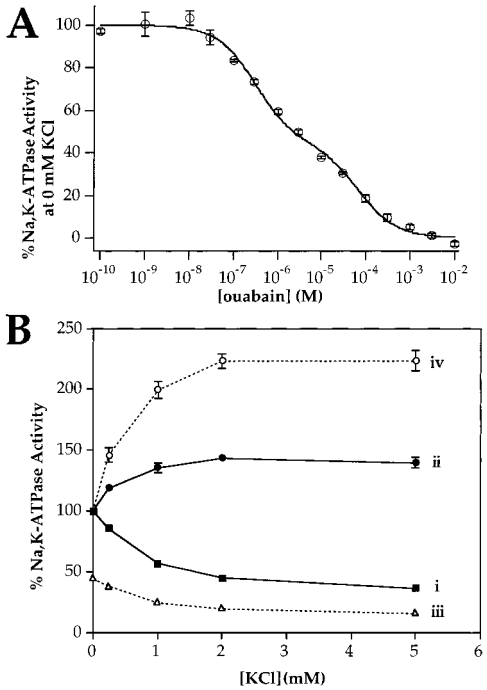

FIGURE 5: Effect of potassium on α2**LN** and α1**RD** activity at 1 μM ATP. Membranes were from the same preparation used to generate panels B and C of Figure 2. (A) Effect of 1 μM ATP and 0 mM KCl on ratio of α1**RD** to α2**LN** Na,K-ATPase activity in membranes prepared from rat muscle. Data were least-squares fitted to a two-component ouabain inhibition curve as described in the legend of Figure 2. Data are means ± SE of three independent measurements and are plotted as a percentage of the total Na,K-ATPase activity defined by the optimal curve fit, 50.15 ± 0.90 nmol of P_i mg^{-1} min^{-1} (mean ± SD). (B) α1**RD** and α2**LN** activity as a function of potassium concentration. Data are means ± SE. (i) % α1**RD** activity in rat kidney membranes, where 100% (n = 6) is 117.69 ± 8.43 nmol of P_i mg^{-1} min^{-1}. (ii) % total Na,K-ATPase (α1**RD** and α2**LN**) activity in rat muscle membranes (n = 9). (iii) % total Na,K-ATPase activity in rat muscle membranes due to α1**RD**, calculated as described in the legend of Figure 4B, using the results of the ouabain titration (part A) combined with the data for the potassium sensitivity of α1**RD** in rat kidney membranes (i). (iv) % α2**LN** activity, determined from the difference between curves ii and iii as described in the legend of Figure 4B.

of 1 μM ATP. In contrast, α2**LN** (iv) undergoes a dramatic activation in response to the addition of potassium, the magnitude of which is much larger than that of the modest activation of α2**RD** by potassium [Figure 5B (iv) vs Figure 4B,C (iii)]. Therefore, the **RD** substitutions appear to alter both the ouabain affinity and the kinetic properties of the α2**LN** isoform.

*Effect of Potassium on Chimeric α1**RD**−α2**RD** Na,K-ATPase Activity at 1 μM ATP*. We were curious about whether inhibition or activation by potassium, like ouabain sensitivity, involved the interaction of the N-terminus and M1−M2 loop with residues located in the remainder of the α subunit. We therefore investigated the potassium sensitivity of four chimeric α1**RD**−α2**RD** subunits. The cDNAs for the various chimeric α subunits (Figure 6A) were constructed using three restriction sites: *Nhe*I (previously described), *Nco*I, and *Afl*III. The *Afl*III and *Nco*I sites are naturally occurring restriction sites located at analogous positions in the two α subunit cDNAs. The *Afl*III site is located near the phosphorylated aspartyl residue (rat α1, bp 1406, H386; rat α2, bp 1261, H384), and the *Nco*I site is located near the

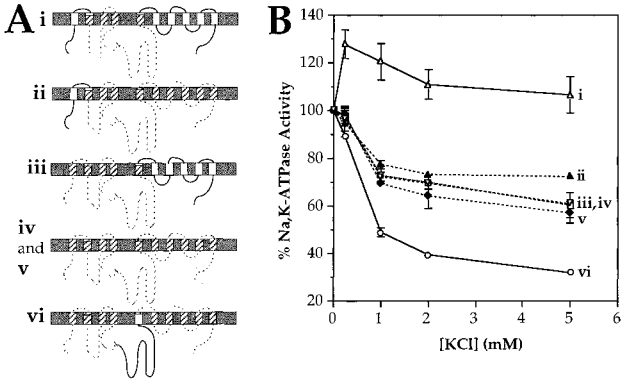

FIGURE 6: Effect of KCl on chimeric α1**RD**−α2**RD** subunits. (A) Chimeric α subunits: (i) α2**RD**NheIα1NcoIα2, (ii) α2**RD**NheIα1, (iii) α1**RD**NcoIα2, (iv) α1**RD**NheI, (v) α1**RD**, and (vi) α1**RD**(NheI)-AflIIIα2NcoIα1. The chimeric α subunits were constructed using three restriction sites: *Afl*III, *Nco*I, and *Nhe*I. The *Afl*III and *Nco*I sites are naturally occurring restriction sites located at analogous positions in the two α subunit cDNAs. The *Afl*III site is located near the catalytic aspartyl residue (rat α1, bp 1406, H386; rat α2, bp 1261, H384), and the *Nco*I site is located near the C-terminus of M5 [rat α1, bp 2435, A729; rat α2, bp 2287, A727; numbering according to Shull et al. (*10*)]. An *Nhe*I site at the N-terminus of M2 (bp 497, flanked by V128 and L129) occurs naturally in the rat α2 subunit cDNA. An analogous *Nhe*I site (bp 643, flanked by V130 and L131) was introduced into the α1 subunit cDNA by site-directed mutagenesis. Creation of the α1 subunit *Nhe*I site results in the substitution S132A, alanine being the residue found at the corresponding position of the α2 subunit. The nomenclature of the various α subunits is as follows. The names of the subunits comprising the various regions of the chimeras and the names of the restriction sites used to join them are listed from the N- to C-terminus. (NheI) indicates that an *Nhe*I site and S132A substitution are present but that the *Nhe*I site was not used to fuse the α1 N-terminus to the rest of the molecule. α2 subunit sequences are depicted as solid lines and white rectangles, whereas α1 subunit sequences are depicted as cross-hatched lines and rectangles. The plasma membrane is indicated in gray, and solid lines denote restriction sites. (B) Effect of KCl on activity of chimeric α subunits at 1 μM ATP. Chimeric α subunit activity as a function of potassium concentration was calculated from the total Na,K-ATPase activity in the presence of 10 μM ouabain as described in the legend of Figure 4C. The total Na,K-ATPase activity in the presence of 10 μM ouabain was determined by subtracting the amount of ATP hydrolyzed in the presence of either 0 mM NaCl or 10 mM ouabain from the amount of ATP hydrolyzed in the presence of 100 mM NaCl and 10 μM ouabain. Data plotted are means ± SE. (i) % α2**RD**NheIα1NcoIα2 activity. The 100% level (n = 6) is 0.200 ± 0.0095 nmol of P_i mg^{-1} min^{-1}. In the absence of potassium and ouabain, the ratio of α1**QN** to α2**RD**NheIα1NcoIα2 activity is 0.683. (ii) % α2**RD**NheIα1 activity. The 100% level (n = 6) is 0.520 ± 0.014 nmol of P_i mg^{-1} min^{-1}. In the absence of potassium and ouabain, the ratio of α1**QN** to α2**RD**NheIα1 activity is 0.272. (iii) % α1**RD**NcoIα2 activity. The 100% level (n = 3) is 0.309 ± 0.020 nmol of P_i mg^{-1} min^{-1}. In the absence of potassium and ouabain, the ratio of α1**QN** to α1**RD**NcoIα2 activity is 0.495. (iv) % α1**RD**NheI activity. The 100% level (n = 6) is 0.891 ± 0.045 nmol of P_i mg^{-1} min^{-1}. In the absence of potassium and ouabain, the ratio of α1**QN** to α1**RD**NheI activity is 0.221. (v) % α1**RD** activity. The 100% level (n = 6) is 0.291 ± 0.0250 nmol of P_i mg^{-1} min^{-1}. In the absence of potassium and ouabain, the ratio of α1**QN** to α1**RD** activity is 0.912. (vi) % α1**RD**(NheI)AflIIIα2NcoIα1 activity. The 100% level (n = 6) is 0.773 ± 0.028 nmol of P_i mg^{-1} min^{-1}. In the absence of potassium and ouabain, the ratio of α1**QN** to α1**RD**(NheI)AflIIIα2NcoIα1 activity is 0.233.

C-terminus of M5 [rat α1, bp 2435, A729; rat α2, bp 2287, A727; numbering according to Shull et al. (*10*)]. For all four of these chimeras, we obtained fairly high numbers of colonies in the presence of 1 μM ouabain (at least ~100 colonies per transfection experiment). In addition, the

cultured colonies grew at rates similar to those of colonies expressing α1**RD** and α2**RD** in media containing 1 μM ouabain (data not shown). We therefore assumed that the ouabain affinities of the various chimeric **RD** subunits were comparable to those of α1**RD** and α2**RD**.

As shown in Figure 6, analysis of these chimeric α subunits reveals that the effect of potassium at low ATP concentrations is determined primarily by the interaction of the N-terminus and M1−M2 loop with the C-terminal third of the α subunit. Substitution of either the C-terminal third [Figure 6A (iii)] or the N-terminus and M1−M2 loop [Figure 6A (ii)] of the α1**RD** subunit with the corresponding pieces of α2**RD** did not significantly alter potassium inhibition [Figure 6B (ii and iii vs iv and v)]. However, a chimera consisting of M2−M5 of the α1 subunit flanked by the N- and C-termini of α2**RD**, α2**RD**NheIα1NcoIα2 (i), was activated by potassium in a manner reminiscent of intact α2**RD** [Figure 4B,C (iii)]. Likewise, α1**RD**(NheI)AflIII-α2NcoIα1 (vi), a chimera consisting of the central third of α2**RD** flanked by the N- and C-terminus of α1**RD**, was inhibited by potassium like the intact α1**RD** subunit [Figures 5B (i) and 6B (v)].

*Effect of Potassium on α2**DR**, α1**DR**, and Chimeric α1**DR**−α2**DR** Na,K-ATPase Activity at 1 μM ATP*. Because the effects of the **DR** substitutions on the ouabain sensitivity of the α1 and α2 isoforms were so extreme and unpredictable (Table 1), we investigated the influence of these substitutions on Na,K-ATPase activity as a function of potassium concentration at low ATP concentrations. As shown in Figure 7, the presence of the combination of residues **DR** at the borders of the M1−M2 loop of both the α1 and α2 subunits profoundly affects Na,K-ATPase activity as a function of potassium concentration. α1ck**DR**NheI (i), in contrast to α1**RD** [Figures 5B and 6B (v)] and α1**RD**NheI [Figure 6B (iv)], is activated by potassium. We were equally surprised to discover that α2ck**DR** (ii), unlike α2**RD** (Figure 4B,C) and α2**LN** (Figure 5B), is essentially completely inhibited by potassium. Our analysis of two α1**DR**−α2**DR** chimeras confirms that inhibition or activation by potassium, like ouabain sensitivity, involves the interaction of the N-terminus and M1−M2 loop with residues located in the remainder of the α subunit. The effect of potassium upon both of the α1**DR**−α2**DR** hybrids (iii and iv) was distinct from its effect on either intact α1ck**DR**NheI (i) or α2ck**DR** (ii). α2ck**DR**NheIα1 (iii) underwent a dramatic activation in response to the addition of potassium, whereas α1ck**DR**NheIα2 remained relatively constant (iv).

In conclusion, the residues at the borders of the M1−M2 loop influence both ouabain and potassium sensitivity in a context-dependent manner.

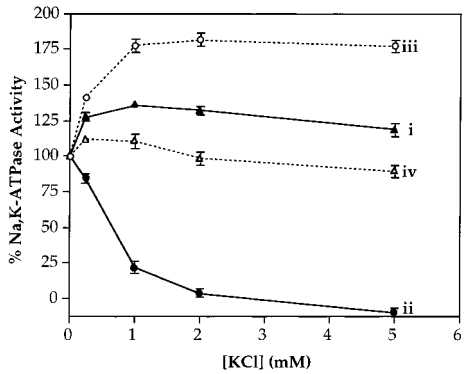

FIGURE 7: Effect of KCl on the Na,K-ATPase activity of α2ck**DR**, α1ck**DR**NheI, and chimeric α1**DR**−α2**DR** subunits at 1 μM ATP. The nomenclature and structure of the various α subunits are described in the legend of Figure 1A. Data are means ± SE. ATP hydrolysis that was not due to the Na,K-ATPase was assessed at 0 mM KCl and 0 mM NaCl. Except for α2ck**DR**, the effect of KCl on the various α subunits was determined as described in the legend of Figure 4C, by subtracting the α1**QN** activity that is resistant to 10 μM at each potassium concentration. Because the ouabain affinities of α2ck**DR** and α1**QN** are very similar, α2**DR** activity as a function of potassium concentration was determined as described in the legend of Figure 4B, by subtracting the α1**QN** activity from the total Na,K-ATPase activity. (i) % α1ck**DR**NheI activity. Data were derived from two ouabain-resistant colonies. The 100% level is 2.600 ± 0.096 nmol of P_i mg^{-1} min^{-1} ($n = 3$) and 0.763 ± 0.025 nmol of P_i mg^{-1} min^{-1} ($n = 5$) for the first and second colony, respectively. In the absence of potassium and ouabain, the ratio of α1**QN** to α1**DR**NheI activity is 0.127 for the first colony and 0.183 for the second. (ii) % α2ck**DR** activity. The 100% level ($n = 6$) is 0.626 ± 0.024 nmol of P_i mg^{-1} min^{-1}. In the absence of potassium and ouabain, the ratio of α1**QN** to α2ck**DR** to total Na,K-ATPase activity is 1.233. (iii) % α2ck-**DR**NheIα1 activity. The 100% level ($n = 6$) is 0.642 ± 0.031 nmol of P_i mg^{-1} min^{-1}. In the absence of potassium and ouabain, the ratio of α1**QN** to α2ck**DR**NheIα1 activity is 0.158. (iv) % α1ck**DR**NheIα2 activity. The 100% level ($n = 6$) is 0.485 ± 0.042 nmol of P_i mg^{-1} min^{-1}. In the absence of potassium and ouabain, the ratio of α1**QN** to α1ck**DR**NheIα2 activity is 1.425.

DISCUSSION

In this study, we compared the effects of two combinations of charged M1−M2 loop border residues, **RD** and **DR**, on ouabain affinity within the context of the rat α1, α2, and three chimeric α1−α2 subunits. We report that the sensitivity of the Na,K-ATPase to inhibition by ouabain is dependent not only upon the identity of the M1−M2 loop border residues but also upon the environment into which they are introduced. Furthermore, the effect of the M1−M2 loop border residues on ouabain sensitivity involves their interaction with other residues located both C-terminal to and within or N-terminal to the M1−M2 loop. This result suggested to us that rather than interacting directly with ouabain, these residues might influence ouabain sensitivity by destabilizing or altering the E2 intermediate of the Na,K-ATPase catalytic cycle to which ouabain binds preferentially (*4*). We proceeded to investigate the effects of substitutions at the M1−M2 loop border on the potassium sensitivity of the Na,K-ATPase at low ATP concentrations, because modifications of regions proximal to the M1−M2 loop have been shown to alter both potassium sensitivity at low ATP concentrations and the E1−E2 conformational equilibrium (*18*, *20*, *23*). In fact, we have found that M1−M2 loop border substitutions can significantly alter potassium sensitivity at low ATP concentrations, and that they do so in a context-dependent manner. To summarize, we have provided additional evidence that the M1−M2 loop border residues influence ouabain sensitivity indirectly, and we have demonstrated that the M1−M2 loop plays an important role in determining the catalytic properties of the Na,K-ATPase.

We found no noticeable correlation between ouabain affinity and the effect of potassium on Na,K-ATPase activity at micromolar ATP concentrations (Table 1 vs Figures 4, 5, and 7). Although we suspect that substitutions at the M1−M2 loop border may influence ouabain affinity by shifting

the E1−E2 conformational equilibrium toward E1, we cannot make firm conclusions in this regard. It has recently been shown that one cannot predict alterations in the E1−E2 equilibrium of the α1 isoform on the basis of changes in potassium sensitivity at micromolar ATP concentrations. Mutations which result in activation of the α1 isoform by potassium at low ATP concentrations have been associated with shifts in the E1−E2 conformational equilibrium toward both E1 (*20*, *23*) and E2 (*18*).

On the basis of the data shown in Figures 6 and 7 and Table 1, we propose that the M1−M2 loop border residues interact with residues located both within the M1−M2 loop and in the C-terminal third of the α subunit. The fact that the **DR** substitutions affect both ouabain sensitivity (Table 1) and potassium sensitivity at low ATP concentrations (Figure 7) in an isoform-dependent manner implies that the effects of M1−M2 loop border substitutions are influenced by other residues which differ in the α1 and α2 subunits. Because the ouabain sensitivity and potassium sensitivity of the α2ck**DR**NheIα1 chimera as well as the potassium sensitivity of the α1ck**DR**NheIα2 chimera are clearly distinct from those of both the intact α2ck**DR** and α1ck**DR**NheI subunits (Table 1 and Figure 7), these other residues are likely to be located both C-terminal to and within or N-terminal to the M1−M2 loop. In fact, the properties of the various chimeric α1**RD**−α2**RD** subunits (Figure 6) suggest that potassium sensitivity is determined primarily by interactions between the N-terminus and M1−M2 loop and the C-terminal third of the α subunit. In the C-terminal third of the α subunit, extracellular residues which vary between the α1 and α2 subunits are located exclusively in the M7−M8 loop (*10*). We therefore hypothesize that the residues within the M1−M2 loop form a domain or surface which interacts directly with the M7−M8 extracellular loop. In fact, mutagenesis of a conserved arginine residue in the M7−M8 loop alters ouabain affinity (*13*). The contacts between the M1−M2 loop and the M7−M8 loop may modulate the rate of the E1−E2 transition and could potentially also influence access of potassium to the cation binding site.

One of the more surprising findings of this study was the dramatic activation of the α2**LN** isoform by potassium in the presence of micromolar ATP concentrations. In intact rat skeletal muscle (*38*, *39*), in contrast to membrane preparations of this tissue [Figure 5, (*39*)], the α2**LN** isoform comprises the vast majority of active Na,K-ATPase molecules. Skeletal muscle acts as a potassium reservoir for the body, and the Na,K-ATPase activity in this tissue plays a central role in determining serum potassium concentrations (*40*, *41*). Activation of α2**LN** by potassium at low ATP concentrations may be crucial to the maintenance of serum and muscle potassium homeostasis under conditions of sustained potassium efflux and ATP depletion such as vigorous exercise or tetanic contraction (*41*). α2**LN** is also expressed in glial cells (*42*), which are thought to play an important role in regulating extracellular potassium levels in the brain (*43*) and retina (*44*). During periods of sustained electrical activity, the capacity of the α2**LN** isoform to be activated by potassium at low ATP concentrations may enable glial cells to maintain a high rate of potassium uptake and thereby prevent nonspecific depolarization of neurons.

Given the fact that the β subunit can influence potassium affinity (*45*), it is also possible that the striking difference between the magnitude of the potassium activation of the α2**RD** (∼30%) and the α2**LN** (∼250%) isoforms may be due to differences in β subunit content in HeLa and rat skeletal muscle cells and not to the presence of the **RD** substitutions. HeLa cells express only the β1 isoform, whereas all three β subunit isoforms have been detected in skeletal muscle (*37*, *46*).

The introduction of the combination of residues **RD** at the borders of the M1−M2 loop has been used as a means to facilitate the study of the properties of the ouabain-sensitive, rat α2 and α3 isoforms in ouabain-sensitive cell lines such as HeLa (*24*). The data presented herein indicate that caution is warranted in assessing the significance of results obtained with α subunits containing substitutions at the borders of the M1−M2 loop. We have shown that M1−M2 loop border substitutions can simultaneously alter both the ouabain sensitivity and the kinetic properties of the Na,K-ATPase. This study in conjunction with that of Arystarkhova et al. (*25*), in which a monoclonal antibody specific to the M1−M2 loop is shown to enhance ouabain binding, points to a potentially critical role for the M1−M2 loop in regulating the conformational shifts which occur throughout the Na,K-ATPase catalytic cycle.

ACKNOWLEDGMENT

We thank Dr. Jerry Lingrel for providing us with the cDNAs for the rat α1 and α2 subunits. We also thank the other members of our laboratory for their assistance and input, especially Lorraine Santy, Alison Grinthal, and Ting Fang Wang.

REFERENCES

1. Lingrel, J. B., and Kuntzweiler, T. (1994) *J. Biol. Chem. 269*, 19659−62.
2. Beguin, P., Wang, X., Firsov, D., Puoti, A., Claeys, D., Horisberger, J., and Geering, K. (1997) *EMBO J. 16*, 4250−60.
3. Shainskaya, A., and Karlish, S. (1994) *J. Biol. Chem. 269*, 10780−9.
4. Jørgensen, P. L., and Andersen, J. P. (1988) *J. Membr. Biol. 103*, 95−120.
5. Price, E. M., Rice, D. A., and Lingrel, J. B. (1990) *J. Biol. Chem. 265*, 6638−41.
6. O'Brien, W. J., Lingrel, J. B., and Wallick, E. T. (1994) *Arch. Biochem. Biophys. 310*, 32−9.
7. Price, E. M., and Lingrel, J. B. (1988) *Biochemistry 27*, 8400−8.
8. Croyle, M., Woo, A., and Lingrel, J. (1997) *Eur. J. Biochem. 248*, 488−95.
9. Shull, G. E., Schwartz, A., and Lingrel, J. B. (1985) *Nature 316*, 691−5.
10. Shull, G. E., Greeb, J., and Lingrel, J. B. (1986) *Biochemistry 25*, 8125−32.
11. Antolovic, R., Schoner, W., Geering, K., Canessa, C., Rossier, B., and Horisberger, J. (1995) *FEBS Lett. 368*, 169−72.
12. Askew, G., and Lingrel, J. (1994) *J. Biol. Chem. 269*, 24120−6.
13. Schultheis, P. J., Wallick, E. T., and Lingrel, J. B. (1993) *J. Biol. Chem. 268*, 22686−94.
14. Canessa, C., Horisberger, J., Louvard, D., and Rossier, B. (1992) *EMBO J. 11*, 1681−7.
15. Abbott, A., and Ball, W. J. (1992) *Biochemistry 31*, 11236−43.

16. Kirley, T., and Peng, M. (1991) *J. Biol. Chem. 266*, 19953−7.
17. Arguello, J. M., and Lingrel, J. B. (1995) *J. Biol. Chem. 279*, 22764−71.
18. Blostein, R., Wilczynska, A., Karlish, S., Arguello, J., and Lingrel, J. (1997) *J. Biol. Chem. 272*, 24987−93.
19. Burns, E., Nicholas, R., and Price, E. (1996) *J. Biol. Chem. 271*, 15879−83.
20. Daly, S. E., Blostein, R., and Lane, L. K. (1997) *J. Biol. Chem. 272*, 6341−7.
21. Wierzbicki, W., and Blostein, R. (1993) *Proc. Natl. Acad. Sci. U.S.A. 90*, 70−4.
22. Daly, S., Lane, L., and Blostein, R. (1994) *J. Biol. Chem. 269*, 23944−8.
23. Daly, S., Lane, L., and Blostein, R. (1996) *J. Biol. Chem. 271*, 23683−9.
24. Jewell, E. A., and Lingrel, J. B. (1991) *J. Biol. Chem. 266*, 16925−30.
25. Arystarkhova, E., Gasparian, M., Modyanov, N., and Sweadner, K. (1992) *J. Biol. Chem. 267*, 13694−701.
26. O'Brien, W. J., Wallick, E. T., and Lingrel, J. B. (1993) *J. Biol. Chem. 268*, 7707−12.
27. Kaufman, R. J., Davies, M. V., Pathak, V. K., and Hershey, J. W. (1989) *Mol. Cell Biol. 9*, 946−58.
28. Coppi, M. V., and Guidotti, G. (1997) *Arch. Biochem. Biophys. 346*, 312−21.
29. Kunkel, T. A., Roberts, J. D., and Zakour, R. A. (1987) *Methods Enzymol. 154*, 367−82.
30. Kozak, M. (1987) *J. Mol. Biol. 196*, 947−50.
31. Peterson, G. L. (1977) *Anal. Biochem. 83*, 346−56.
32. Barchi, R. L., Weigele, J. B., Chalikian, D. M., and Murphy, L. E. (1979) *Biochim. Biophys. Acta 550*, 59−76.
33. Jørgensen, P. L. (1974) *Biochim. Biophys. Acta 356*, 53−67.
34. Lanzetta, P. A., Alvarez, L. J., Reinach, P. S., and Candia, O. A. (1979) *Anal. Biochem. 100*, 95−7.
35. Pressley, T. A., Haber, R. S., Loeb, J. N., Edelman, I. S., and Ismail-Beigi, F. (1986) *J. Gen. Physiol. 87*, 591−606.
36. Burgener-Kairuz, P., Horisberger, J., Geering, K., and Rossier, B. (1991) *FEBS Lett. 290*, 83−6.
37. Hundal, H. S., Marette, A., Mitsumoto, Y., Ramlal, T., Blostein, R., and Klip, A. (1992) *J. Biol. Chem. 267*, 5040−3.
38. Clausen, T., and Hansen, O. (1977) *J. Physiol. 270*, 415−30.
39. Hsu, Y. M., and Guidotti, G. (1991) *J. Biol. Chem. 266*, 427−33.
40. DeFronzo, R. A., and Bia, M. (1985) in *The Kidney, Physiology and Pathophysiology* (Seldin, D. W., and Giebisch, G., Eds.) pp 1179−206, Raven, New York.
41. Clausen, T. (1990) *News Physiol. Sci. 5*, 148−51.
42. McGrail, K. M., Phillips, J. M., and Sweadner, K. J. (1991) *J. Neurosci. 11*, 381−91.
43. Amedee, T., Robert, A., and Coles, J. (1997) *Glia 21*, 46−55.
44. Kusaka, S., and Puro, D. G. (1997) *J. Physiol. 500*, 593−604.
45. Jaisser, F., Jaunin, J., Geering, K., Rossier, B. C., and Horisberger, J. D. (1994) *J. Gen. Physiol. 103*, 605−23.
46. Arystarkhova, E., and Sweadner, K. J. (1997) *J. Biol. Chem. 272*, 22405−8.

BI982180J